Theoretical study of double-resonance processes in the helium continuum

Alessandro Lami
Istituto di Chimica Quantistica ed Energetica Molecolare del Consiglio Nazionale delle Ricerche, Via Risorgimento 35, I-56126 Pisa, Italy

Naseem K. Rahman
Dipartimento di Scienze Chimiche, Università di Trieste, Piazzale Europa 1, I-34100 Trieste, Italy

Pietro Spizzo
Istituto di Chimica Quantistica ed Energetica Molecolare del Consiglio Nazionale delle Ricerche, Via Risorgimento 35, I-56126 Pisa, Italy

(Received 22 March 1989)

The ionization spectrum of the He atom under double-resonance irradiation is studied theoretically. A previously developed theory is extended and adapted to treat this process. The first source (synchrotron) is tuned around the transition from the ground state to the $23sp-{}^1P^o$ autoionizing state, and the second source (laser) is put in resonance with the transition from $23sp-{}^1P^o$ to the higher-lying quasibound state $2p3p\ {}^1P^e$ (or $2p4p$, $2p5p$). Accurate *ab initio* calculations have been performed to obtain all the necessary parameters. It is found that the single-field ionization spectrum is strongly modified, exhibiting coherent trapping and ac Stark splitting. These results are in consonance with previous model calculations as well as with other *ab initio* calculations on a different zone of the He continuum. The results show that for the resonances considered these strong effects can be observed at megawatt laser intensities.

I. INTRODUCTION

Two independent external electromagnetic fields are essential for a class of atomic and molecular physics experiments. This consists of those experiments in which one of the two fields is utilized to perturb the isolated atom (molecule), and the second external field probes this perturbed system. Double-resonance spectroscopy is based on such a concept and has proved to be of much utility for understanding the interaction of atoms (molecules) with external electromagnetic fields.[1]

This area of research has acquired an additional dimension in recent years with the continuum taken explicitly into account. Previously, all double-resonance schemes considered only discrete states of a system. The frequencies of the electromagnetic fields matched the discrete energy intervals of the system in question with all the relevant states being in the discrete part of the spectrum. What happens if one of the three levels necessary to consider a double resonance experiment is squarely in the continuum, has aroused the interest of many researchers.[2–11] One of the principal reasons for this is that the continuum in such a scheme allows one to consider various new phenomena, such as the creation of a photon-dressed stabilized state or even a pair of such states. The interference effects that are produced due to the presence of autoionizing states in the continuum lead to considerations of the analogue of coherent trapping,[12] by now well understood both theoretically and experimentally. In molecular physics, the predissociating states may give rise to interesting pathways of selective and efficient photodissociation.[4] The opportunities offered by the introduction of the continuum are not yet completely explored, as would appear from the attention that is still being paid by the theoretical research in this area.

One of the aspects of this newer kind of spectroscopy is, however, the lack of accurate calculations with specific atoms or molecules. Most of the works reported concern theoretical models rich in ideas but somewhat meager in terms of quantitative predictions, the reason for which is to be sought in the absence of *ab initio* calculations so necessary for quantitative predictions. An exception is a recent work on helium, where accurate *ab initio* calculations have been utilized to bring the theory to the consideration for experimental realization.[13] In this paper, we also consider helium, albeit with a different *ab initio* calculation and in a different energy regime, in order to understand some of the theoretical constructs in an experimental setting. These two works, along with, hopefully, more to come, should allow one to propose helium for considerations of experiment, especially since helium, apart from being one of the easiest atoms to work with experimentally, lends itself to reliable *ab initio* calculations better than any other atomic system.

The experimental motivation for such research is also not too difficult to see. The possibility of having simultaneous beams of photons arising from a laser and a synchrotron for two-photon experiments is a rather enticing prospect for not far in the future. Already, lasers are utilized to excite atomic systems which are then photoionized by synchrotrons.[14] Furthermore, in solids, photons from a synchrotron and a laser haver been utilized for joint excitation.[15] The capability of having a monochromatic polarized light source in the energy range

where autoionizing states may be coupled directly to the ground state, i.e., by a single photon, and the development of lasers with which such autoionizing states may be coupled to other states that one wants to "strong couple," make the necessity of such calculations evident in order to be able to evaluate the outcomes of such experiments.

The purpose of the scheme investigated in this work is to excite the system from the ground state to the $^1P^o$ continuum in the energy range of the first narrow autoionizing state, the $23sp-{}^1P^o$ state and then to couple this state to a $2pnp\ ^1P^e$ one (see Refs. 16–20 and references therein). These states lie above the $n=1$ ionization threshold, but the $^1P^e$ continuum opens only at the $n=2$ threshold, so they may be considered stable against autoionization, which may occur only through exceedingly weak interactions (i.e., spin orbit and mass polarization). The calculations refer to the case in which a $m=0$ photon beam is employed to excite the system and a $m=1$ one to couple the autoionizing level with the $2pnp$ states (two-photon) transitions between $^1S^e$ and $^1P^e$ manifolds are forbidden if the photons have the same polarization).

The following sections contain a description of the *ab initio* calculations for helium that have been used to construct the effective Hamiltonian and a presentation of the theory adapted for the process in question. This is followed by the results of the calculation of the photoelectron spectra, the final observable of such processes. We find that our results make the prospects of such experiments rather attractive due to the low laser intensities required. These are then discussed and some relevant conclusions are drawn.

II. WAVE FUNCTIONS AND MATRIX ELEMENTS

The method of calculation has been discussed in detail elsewhere,[16] so here only the main features are summarized. Unless otherwise specified, all quantities are expressed in atomic units.

In helium the LS coupling is quite adequate, so the states may be characterized by the usual labels n, L, M_L, S, M_S, and π (parity) and only the $M_L=M_S=0$ components need to be calculated.

The states needed in this calculations have been obtained by large configuration-interaction CI expansions over L^2 bases formed by spin- and symmetry-adapted Slater determinants

$$N_{qq'}\sum_m C(ll'Lm-m0)(|\chi_{qlm}\alpha\chi_{q'l'-m}\beta| - |\chi_{qlm}\beta\chi_{q'l'-m}\alpha|)$$

where N_{qq} is a normalization constant and the basis orbitals χ_{qlm} belong to the following types: (a) Slater-type orbitals (STO), needed to describe the wave functions in the region close to the nucleus; (b) hydrogenic orbital (HO), needed to represent the outer part of the Rydberg states; (c) simulations of inverse R times a cosinus (SIRC),

$$\chi_{lm}(r)=N_{kl}f_l(r)\cos(kr)Y_{lm}(r)\ ,$$

where $f_l(r)$ is a smooth function of the form

$$f_l(r)=r^l[A\exp(-ar)+B\exp(-br)]\ ,$$

which behaves like r^l for small r and simulates the proper $1/r$ damping of a continuum wave in the interval $2-3<r<80-90$. The k values are chosen equally spaced according to $k_j=(2j+1)\pi/2R_0$, $R_0=200$, so that all the SIRC's have a node in R_0. As shown in previous work, by employing a large number of basis configurations of the form (φ_{1S}) (HO,SIRC) corresponding to a large R_0, it is possible to obtain many "continuum" variational wave packets that are almost exactly proportional to the true eigenstates of the same energy inside a sphere of radius about R_0. Since in a large outer region of this sphere, the states assume their asymptotic behavior, the proportionality constants and phase shifts of the variational states may be obtained by comparing the calculated electron waves to $\delta(E)$-normalized shifted Coulomb waves. Since all the matrix elements required in this work involve at least one localized state, the variational states normalized in this way reproduce them accurately. Although a single calculation may yield only a point in the energy region of a narrow resonance, it is possible to reproduce in detail the behavior of the phase shift and of the photoionization cross section by performing several calculations for slightly different values of R_0. The resonance width Γ and the Fano parameter q have been obtained in a previous work[16] by a least-squares fit of the phase shift and of the photoionization cross section to their theoretical expressions.

The initial state, the ground state $1s^2\,^1S^e$, and the final states $2pnp\ ^1P^e$ are the lowest of their symmetries; their approximation through CI wave functions needs no more specifications, although a few comments may be appropriate.

Our ground-state wave function does not reach the extreme accuracy of more refined calculations, but its energy $-2.903\,53$ compares well with the "exact" nonrelativistic value $-2.903\,72$ (Ref. 17) and yields oscillator strengths and photoionization cross sections in excellent agreement with theory and experiment. On the whole, any error in the initial state is well below the other approximations involved in the present work.

The energies of the $2pnp\ ^1P^e$ levels, $-0.580\,22$, $-0.540\,03$, and $-0.524\,09$, compare well with the available experimental and theoretical data.[18–20]

Finally, a localized representation of the $23sp-{}^1P^o$ resonance has been obtained by diagonalizing the Hamiltonian over a basis including localized and Rydberg orbitals but no SIRC ones. The interaction with the continuum displaces this state by about 3×10^{-6}, fully comparable with its width 3.985×10^{-6}. Position, width, and q parameter of this resonance are in good agreement with the available data.

The transition-matrix elements have been computed with both the length and the velocity form of the dipole operator showing good gauge invariance. Only the length-gauge results have been utilized for the computations.

The atomic parameters utilized are summarized in Table I.

TABLE I. Relevant parameters of the He states in Fig. 1 as obtained from the *ab initio* calculations discussed in the text (all in atomic units).

State	Energy	n	T_n
$1s^2\,{}^1S^e$	−2.903 53	3	2.491
$23sp-\,{}^1P^o$	−0.597 00	4	0.3151
$2p3p\,{}^1P^e$	−0.580 22	5	0.1783
$2p4p\,{}^1P^e$	−0.540 03		
$2p5p\,{}^1P^e$	−0.524 09		

$$T_n=\langle 2pnp\,{}^1P^e,\ m=1|r_+|23sp-\,{}^1P^o,\ m=0\rangle$$
$$\gamma_2=1.89\times10^{-6},\quad q_2\equiv q=-4.0$$
$$\sigma(\bar\omega)=\sigma_a\frac{(q+\bar\omega)^2}{1+\bar\omega^2},\quad \bar\omega=\omega/\gamma_2$$
$$\sigma_m=\sigma_a(q^2+1)=0.708$$

III. THEORY

The photoionization rate of the atom, according to the scheme depicted in Fig. 1, can be computed utilizing the effective Hamiltonian approach developed in previous papers[4] and using the results of the *ab initio* computations previously described. The difference with our previous work lies in the fact that here, the autoionizing resonance is the intermediate state, whereas in the past we focused on the case of a resonance as the vertex of a Λ scheme. Such a difference is, however, of minor importance from the point of view of the theory.

Let us recall the essential features of our treatment.[4] The first step consists in considering each autoionizing resonance as the result of the interaction of a bound state with a continuum. As a consequence, we have to consider a flat continuum i.e., one for which the relevant matrix elements are weakly energy dependent.

The next step is the examination of the full Hamiltonian for an atom plus two single-mode fields (ω_1,ω_2) and the selection of the relevant resonant subspace. For the present case, such subspace is assumed to be the one spanned by the following atom times photon states (see Fig. 1 for a visual guide):

$$\begin{aligned}&|1{:}n_1,n_2\rangle\ ,\\ &|2;n_1-1_1n_2\rangle;\{|\varepsilon_\alpha;n_1-1,n_2\rangle\}\ ,\\ &|3;n_1-1,n_2-1\rangle;\{|\varepsilon_\beta;n_1-1,n_2-1\rangle\}\ ,\\ &\{|\varepsilon_\beta;n_1-1,n_2-2\rangle\}\ .\end{aligned}\tag{1}$$

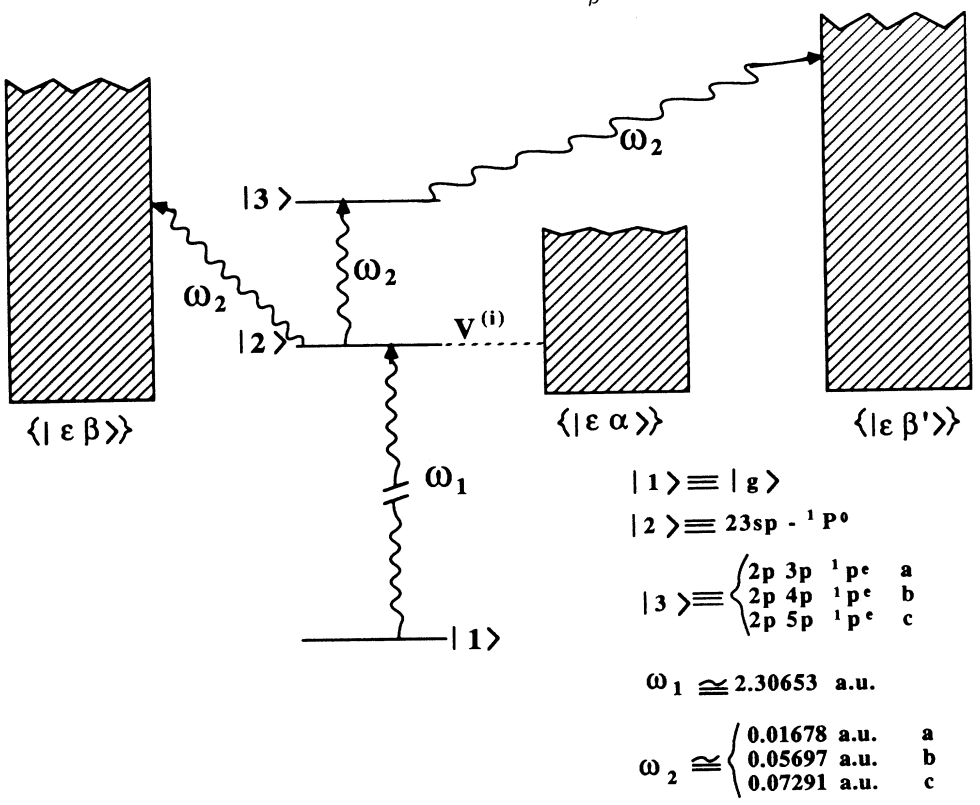

FIG. 1. The ground state and the part of the continuum spectrum of the helium atom utilized for the double-resonance scheme. The states are indicated by the dominant configuration. According to the present *ab initio* calculation, $|3\rangle$ is a nearly stable state embedded in the continuum for all the three cases indicated in the figure. Also shown are the various photon emission-absorption processes taken into account in the present work. The absorption of more than one photon ω_1 is neglected since we study the limit of weak intensity. The second source ω_2 is assumed to be not so strong as to allow a significant continuum-continuum absorption emission.

While all the states in (1) are globally quasidegenerate, only those on the same line have nearly the same atomic energy. The choice of the subspace (1) means that we are taking into account (1) transitions from the ground state $|1\rangle$ to the state $|2\rangle$ or direct ionization into the continuum $\{|\varepsilon_\alpha\rangle\}$ (which interacting with $|2\rangle$ gives rise to the resonance) by absorption of a photon ω_1; (2) transition from $|2\rangle$ to $|3\rangle$ by absorption of a photon ω_2; (3) ionization from $|2\rangle$ to $\{|\varepsilon_\beta\rangle\}$ (a continuum degenerate with $|3\rangle$ but not interacting with it) by absorption of ω_2; (4) ionization from $|3\rangle$ to $\{|\varepsilon_{\beta'}\rangle\}$ by absorption of ω_2.

We have neglected continuum-continuum transition as well as those that involve more than one photon ω_1 (this latter omission is due to the fact that we are interested in a weak ω_1 field). As shall be seen *a posteriori*, the field strength of ω_2 for the experiment lies in the megawatt range, making the effect of the continuum-continuum transitions of imperceptible proportion. We have also treated $|3\rangle$ as a stable state.

The zero order states (1) are couplied by the two electromagnetic fields as well as by the internal perturbation $V^{(i)}$ responsible for autoionization. According to the previous assumptions, we write the Hamiltonian as (the notation is contracted, for simplicity: $|1;n_1,n_2\rangle \equiv |1\rangle$, etc.)

$$
\begin{aligned}
H=&(\varepsilon_1+n_1\omega_1+n_2\omega_2)|1\rangle\langle 1|+[\varepsilon_2+(n_1-1)\omega_1+n_2\omega_2]|2\rangle\langle 2|+[\varepsilon_3+(n_1-1)\omega_1+(n_2-1)\omega_2]|3\rangle\langle 3| \\
&+\sum_\mu \int \varepsilon_\mu|\varepsilon_\mu\rangle\langle\varepsilon_\mu|d\varepsilon_\mu+(V_{12}^{(1)}|1\rangle\langle 2|+\text{H.c.})+(V_{23}^{(2)}|2\rangle\langle 3|+\text{H.c.})+\left[\int V_{1\varepsilon_\alpha}^{(1)}|1\rangle\langle\varepsilon_\alpha|d\varepsilon_\alpha+\text{H.c.}\right] \\
&+\left[\int V_{2\varepsilon_\beta}^{(2)}|2\rangle\langle\varepsilon_\beta|d\varepsilon_\beta+\text{H.c.},\right]+\left[\int V_{2\varepsilon_\alpha}^{(i)}|2\rangle\langle\varepsilon_\alpha|d\varepsilon_\alpha+\text{H.c.}\right]+\left[\int V_{2\varepsilon_\beta}^{(2)}|2\rangle\langle\varepsilon_\beta|d\varepsilon_\beta+\text{H.c.}\right] \\
&+\left[\int V_{2\varepsilon_{\beta'}}^{(2)}|2\rangle\langle\varepsilon_{\beta'}|d\varepsilon_{\beta'}+\text{H.c.}\right], \qquad (2)
\end{aligned}
$$

where

$$
V^{(1)}=-\boldsymbol{\mu}\cdot\mathbf{E}_1, \quad V^{(2)}=-\boldsymbol{\mu}\cdot\mathbf{E}_2 .
$$

We proceed now by projecting out all the continua involved in the subspace (1) and obtain the following 3×3 effective Hamiltonian matrix:

$$
H^{\text{eff}}\equiv\begin{bmatrix} -i\gamma_1+\Delta & (\gamma_1\gamma_2)^{1/2}(q-i) & 0 \\ (\gamma_1\gamma_2)^{1/2}(q-i) & -i\gamma_2 & V_{23}^{(2)} \\ 0 & V_{23}^{(2)} & -i\gamma_3+\Delta' \end{bmatrix}, \qquad (3)
$$

where

$$
\begin{aligned}
&\gamma_1\equiv\gamma_1^\alpha, \quad \delta_1\equiv\delta_1^\alpha , \\
&\gamma_2\equiv\gamma_2^\alpha+\gamma_2^\beta, \quad \delta_2=\delta_2^\alpha+\delta_2^\beta , \\
&\gamma_3\equiv\gamma_3^{\beta'} , \\
&\gamma_1^\alpha=\pi|V_{1\varepsilon_\alpha}^{(1)}|^2 , \\
&\gamma_2^\alpha=\pi|V_{2\varepsilon_\alpha}^{(i)}|^2, \quad \gamma_2^\beta=\pi|V_{2\varepsilon_\beta}^{(2)}|^2 , \\
&\gamma_3^{\beta'}=\pi|V_{3\varepsilon_{\beta'}}^{(2)}|^2 . \qquad (4)
\end{aligned}
$$

The real part of the level shift δ is given by the Hilbert transform of the corresponding γ; for example,

$$
\delta_1^\alpha=\frac{1}{\pi}P\int\frac{\gamma_1^\alpha}{E-\varepsilon_\alpha}d\varepsilon_\alpha, \text{ etc.} \qquad (5)
$$

The Fano parameter q is defined as usual:

$$
q=\left[V_{12}^{(1)}+\frac{1}{\pi}P\int\frac{V_{1\varepsilon_\alpha}^{(1)}V_{\varepsilon_\alpha 2}^{(i)}}{\varepsilon_2-\varepsilon_\alpha}d\varepsilon_\alpha\right](\gamma_1^\alpha\gamma_2^\alpha)^{-1/2} . \qquad (6)
$$

The two detunings in Eq. (3) are defined as

$$
\begin{aligned}
&\Delta=\varepsilon_1+\delta_1+\omega_1-(\varepsilon_2+\delta_2) , \\
&\Delta'=\varepsilon_3+\delta_3-(\varepsilon_2+\delta_2+\omega_2) . \qquad (7)
\end{aligned}
$$

The effective Hamiltonian (3) is the starting point for computing the relevant transition amplitudes between $|1\rangle$, $|2\rangle$, and $|3\rangle$, which are the basic ingredients for evaluating the ionization rate into the various channels (see the Appendix). A compact expression for the ionization rate for the case of a weak ω_1 field is derived in the Appendix. In the limit of very weak ω_1 field one has

$$
\begin{aligned}
&W_\alpha\cong 2\gamma_1\left[1+\gamma_2\frac{[2qS+(q^2-1)P]}{S^2+P^2}\right] , \\
&W_\beta\cong 0 , \\
&W_{\beta'}\cong 0
\end{aligned}
$$

[S and P are given in (A22) and (A23)]. Notice that the above ionization rate W_α depends linearly on the intensity of the ω_1 field (since $\gamma_1\propto|E_1|^2$) but is a highly nonlinear function of $|E_2|^2$. The above expressions have been used to perform the calculations on helium atom presented and discussed in Sec. IV. [Equations (A27) could be used to investigate the case of weak to moderate ω_1 field.]

IV. RESULTS AND DISCUSSIONS

We shall now examine the result of the computations for the helium atom in the region of the $23sp-$ resonance (state $|2\rangle$ in Fig. 1). In Fig. 2, the double-resonance ionization spectrum for the electron emerging around the energy $E_2-\varepsilon_\alpha^{\text{thresh}}$ (ε_α is the continuum involved in the autoionizing state) is shown. The second field ω_2 is tuned to match the energy of the upper (long-lived) resonance

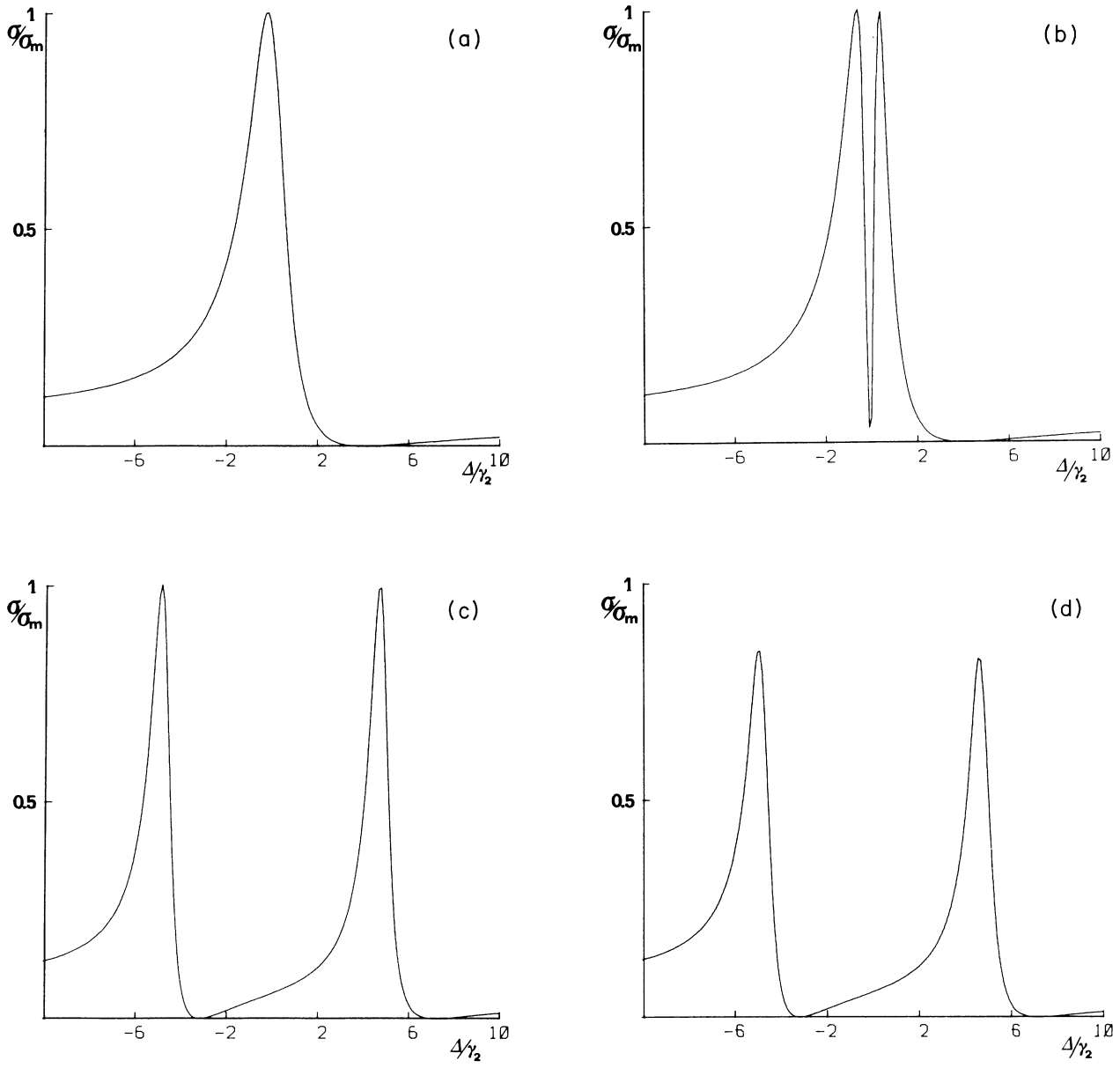

FIG. 2. (a) Fano line shape for the ionization from the helium ground state for ω_1 close to the excitation energy of the resonance $23sp-$. The values of q and γ_2^a have been obtained by fitting the *ab initio* calculations: $q=-4$, $\gamma_2^a=1.89\times10^{-6}$ a.u. (Table I). The abscissa is the detuning Δ [see Eq. (7)] in units of γ_2^a i.e., Δ/γ_2^a. The ordinate is the ionization cross section in units of its maximum value, i.e., σ_m. Since the *ab initio* calculation gives $\sigma_m=0.708$, the value of σ may be easily extracted from the figure. (b) Ionization cross section when the second field ω_2 is switched on. The units are the same as in (a) (σ_m is again the maximum value of σ when only ω_1 is switched on). Here $|3\rangle=2p3p$ and $I_2=10^5$ W/cm^2. (c) Same as in (b) with $I_2=10^6$ W/cm^2. (d) In the previous cases, the ionization from level $|3\rangle$ into the continuum $\{|\varepsilon_{\beta'}\rangle\}$ by absorption of a photon ω_2 has been neglected. Here we mimic the effect of this additional channel by assuming $\gamma_3^{\beta'}=\gamma_2^a/10$. The intensity I_2 is the same as in (c).

$2p3p$ (see Fig. 1) and its intensity is progressively increased starting form $I_2=0$ [Fig. 2(a)] to $I_2=10^6$ W/cm^2 [Fig. 2(c)].

Here we have neglected the ionization up from level $|2\rangle$ into the continuum $\{|\varepsilon_\beta\rangle\}$ and from level $|3\rangle$ into the continuum $\{|\varepsilon_{\beta'}\rangle\}$ by absorption of a photon ω_2. We have estimated that the probability of such process with respect to the primary one (ionization in α) is negligible for $I_2<10^8$W/cm^2) i.e., for all the cases computed.

Figure 2 shows the typical features of a double-resonance spectrum (see Ref. 4 for a discussion on similar absorption spectra for model systems). The ω_2 field produces a very narrow dip for small values of the intensity I_2. This effect can be attributed to a coherent trapping

effect (see Ref. 1). By increasing the I_2, the dip broadens and the peaks move apart, due to the dynamical Stark splitting originating from the strong field-induced coupling between the $2pnp$ and the $23sp-$ resonance.

Figures 2(b)–2(c) refer to the case in which $|3\rangle \equiv 2p3p\ ^1P^e$. It is, however, worthwhile to note that they are far more general as far as the choices of $|3\rangle$ are concerned. In fact, any other long-lived level (and, in particular, the other two obtained here from the *ab initio* calculation, i.e., $2p4p$ and $2p5p$) exhibits the same behavior at a scaled intensity. Suppose that utilizing a given state $|3\rangle$ with the transition moment μ we have computed the ionization spectrum at a certain intensity I. Then it is easy to verify that the same spectrum holds for another state $|3\rangle$ with μ' at the scaled intensity $I'=I(\mu/\mu')^2$. Hence the same Figs. 2(b) and 2(c) can be referred to $|3\rangle = 2p4p$, with intensities $62.5I_2$ and $195.2I_2$ respectively.

Looking at Figs. 2(b) and 2(c) one can see that the intensity required to observe a drastic modification of the ionization spectrum is not very high (and several orders of magnitudes less than one needed for the case studied in Ref. 13). The reason is that we have focused on an intermediate resonance (i.e., the state $|2\rangle = 23sp-$) having a quite long lifetime $1/\gamma_2$ (in fact the ionization spectrum undergoes a strong modification only when $V_{23}^2/\gamma_2 \sim 1$).

As a conclusion, we briefly review the content of the paper. We have presented the scheme for the double-resonance experiment in the continuum of an atomic system, specializing ourselves for the helium atom, with the support of appropriate *ab initio* calculations. We have calculated the ionization spectrum when the helium atom in its ground state is simultaneously irradiated with a weak light source ω_1 such that it is ionized near the $23sp-$ resonance and a stronger source ω_2 to match the energy difference between the above resonance and the upper level $2p3p\ ^1P^e$ (or $2p4p$, $2p5p$). We have shown that significant effects appear at intensities around 10^6 W/cm^2. This intensity value in rather promising for an experimental realization, since it is still sufficiently weak to maintain at a negligible level other photon absorption-emission processes which could obscure the one we are interested in. Therefore we believe that this is the zone of the helium continuum that merits particular attention for the experimental realization of a double-resonance ionization using ω_1 photons from a synchrotron and ω_2 photons from a laser.

APPENDIX

We derive here an expression for the number of electrons at time t into the various continua, in the limit of weak ω_1 field. We call $P(t)$ the number of electrons and use the same label for the continua as in Fig. 1. Hence, for example, $P_\alpha(t)$ is the number of electrons ionized into the continuum α at time t, etc. The various P's can be calculated from the following relations:

$$P_\beta(t)=2\gamma_2^\beta\int_0^t P_2(t')dt' , \tag{A1}$$

$$P_{\beta'}(t)=2\gamma_3^{\beta'}\int_0^t P_3(t')dt' , \tag{A2}$$

$$P_\alpha(t)=1-P_1(t)-P_3(t)-P_\beta(t)-P_{\beta'}(t) , \tag{A3}$$

where

$$P_1(t)=|U_{11}(t)|^2,\quad P_3(t)=|U_{31}(t)|^2 . \tag{A4}$$

The above equations refer to the specific case of He discussed in this paper, since the autoionizing width of the state $|3\rangle$ has been assumed to be negligible.

The transition amplitudes $U_{j1}(t)$ can be easily computed from the relation

$$U_{j1}(t)=\frac{1}{2\pi i}\oint\left\langle j\left|\frac{e^{-izt}}{z-H^{\text{eff}}}\right|1\right\rangle dz \tag{A5}$$

through the residue theorem. Indicating by M_{1j} the cofactor of $(z-H^{\text{eff}})_{1j}$ and by z_0, z_1, and z_2, the three roots of the secular equation, one has

$$U_{j1}(t)=a_j e^{-iz_0 t}+b_j e^{-iz_1 t}+c_j e^{-iz_2 t} , \tag{A6}$$

where

$$\begin{aligned} a_j &= M_{j1}(z_0)/(z_0-z_1)(z_0-z_2) , \\ b_j &= M_{j1}(z_1)/(z_1-z_0)(z_1-z_2) , \\ c_j &= M_{j1}(z_2)/(z_2-z_0)(z_2-z_1) . \end{aligned} \tag{A7}$$

In the limit of weak ω_1 field, one of the roots, say z_0, is essentially the unperturbed complex energy $\Delta-i\gamma_1$ with a small correction. The other two roots z_1 and z_2 have a much larger imaginary part. Hence after a rapid transient, Eq. (A5) becomes

$$U_{j1}(t)\cong a_j e^{-it_0 t} \tag{A8}$$

and

$$|U_{ij}(t)|^2 \cong A_j e^{-2\Gamma_0 t} , \tag{A9}$$

where

$$\begin{aligned} \Gamma_j &= -\text{Im}(z_j) , \\ A_j &= |a_j|^2 . \end{aligned} \tag{A10}$$

Equations (A8) and (A9) are valid for $t \gg \Gamma_1^{-1}, \Gamma_2^{-1}$.

Let us consider the ionization by a pulse of duration $t_p \gg \Gamma_1^{-1}, \Gamma_2^{-1}$ and suppose that we are able to collect all the electrons ionized from $t=0$ to essentially $t=\infty$. The collected number of electrons is indicated by $\mathcal{N}$. One has (N is the number of atoms in the interaction volume)

$$\begin{aligned} \mathcal{N}_\beta &= NP_\beta(t_p) , \\ \mathcal{N}_{\beta'} &= NP_{\beta'}(t_p) , \\ \mathcal{N}_\alpha &= N[1-P_1(t_p)-P_3(t_p)]-\mathcal{N}_\beta-\mathcal{N}_{\beta'} . \end{aligned} \tag{A11}$$

Notice that all the $\mathcal{N}$'s except $\mathcal{N}_\alpha$ are simply proportional to the corresponding P at the end of the pulse. The reasons for the peculiarity of $\mathcal{N}_\alpha$ is that all the population that, at the end of the pulse, was in state $|2\rangle$ is fully ionized after a sufficient time.

Let us now evaluate the P's. From Eqs. (A1)–(A3) and (A9), we have, for $t_p \ll 1/\Gamma_0$, i.e., far from saturation (for the field ω_2),

$$P_\beta(t_p)\cong 2\gamma_2^\beta A_2\frac{1-e^{-2\Gamma_0 t_p}}{2\Gamma_0}\cong 2\gamma_2^\beta A_2 t_p\ ,$$
$$P_{\beta'}\cong 2\gamma_3^{\beta'} A_3 t_p\ . \tag{A12}$$

Furthermore,

$$P_1(t_p)\cong A_1(1-2\Gamma_0 t_p)\ ,$$
$$P_3(t_p)\cong A_3(1-2\Gamma_0 t_p)\ . \tag{A13}$$

The last of Eqs. (A11) becomes

$$\mathcal{N}_\alpha\cong N[1-A_1-A_3+2\Gamma_0 t_p(A_1+A_3) -2\gamma_2^\beta A_2 t_p-2\gamma_3^{\beta'} A_3 t_p]\ . \tag{A14}$$

The term $1-A_1-A_2-A_3$ must be zero since $\mathcal{N}_\alpha(t_p=0)=0$. Hence

$$\mathcal{N}_\alpha\cong 2N[\Gamma_0(A_1+A_3)-\gamma_2^\beta A_2-\gamma_3^{\beta'} A_3]t_p\ . \tag{A15}$$

Defining an ionization rate per atom in the continuum α as

$$W_\alpha=\mathcal{N}_\alpha/(t_p N)\ , \tag{A16}$$

one has

$$W_\alpha\cong 2\Gamma_0(A_1+A_3)-2\gamma_2^\beta A_2-2\gamma_3^{\beta'} A_3\ . \tag{A17}$$

Similarly,

$$W_\beta\cong 2\gamma_2^\beta A_2\ ,$$
$$W_{\beta'}\cong 2\gamma_3^{\beta'} A_3\ . \tag{A18}$$

The final step for obtaining a compact expression for the ionization rate consists in evaluating Γ_0, A_1, A_2, and A_3. The secular equation for H^{eff} can be written as

$$z=\Delta-i\gamma_1+\frac{\gamma_1\gamma_2(q-i)^2}{z+i\gamma_2-V_{23}^2/(z-\Delta'+i\gamma_3)}\ . \tag{A19}$$

An approximate expression for z_0 can be obtained by putting $z=\Delta$ on the right:

$$z_0\simeq\Delta-i\gamma_1+\frac{\gamma_1\gamma_2(q-i)^2}{\Delta+i\gamma_2-V_{23}^2/(\Delta-\Delta'+i\gamma_3)}\ . \tag{A20}$$

Then

$$\Gamma_0=-\mathrm{Im}z_0\cong\gamma_1\left[1+\gamma_2\frac{2qS+(q^2-1)P}{S^2+P^2}\right]\ , \tag{A21}$$

where

$$S=\frac{\Delta-V_{23}^2(\Delta-\Delta')}{(\Delta-\Delta')^2+\gamma_3^2}\ , \tag{A22}$$

$$P=\gamma_2+\frac{V_{23}^2\gamma_3}{(\Delta-\Delta')^2+\gamma_3^2}\ . \tag{A23}$$

From the first of Eqs. (A7), and Eq. (A10), after some passages one obtains (utilizing $z_0\cong\Delta$)

$$A_1=\{[\Delta(\Delta-\Delta')-\gamma_2\gamma_3-V_{23}^2]^2 +[\gamma_2^2(\Delta-\Delta')+\gamma_3\Delta]^2\}/Q\ , \tag{A24}$$

$$A_2=\{\gamma_1\gamma_2[q(\Delta-\Delta')+\gamma_3]^2+(\gamma_3 q-\Delta+\Delta')^2\}/Q\ , \tag{A25}$$

$$A_3=\gamma_1\gamma_2(q^2+1)V_{23}^2/Q\ , \tag{A26}$$

and

$$Q=|(\Delta-z_1)(\Delta-z_2)|^2\ .$$

A combination of Eqs. (A16)–(A18) with Eqs. (A24)–(A27), gives an analytical expression for the ionization rate W as a function of the other two roots z_1 and z_2 of the secular equation (A19):

$$W_\beta=2\gamma_2^\beta\{[\Delta(\Delta-\Delta')-\gamma_2\gamma_3-V_{23}^2]^2 +[\gamma_2(\Delta-\Delta')+\gamma_3\Delta]^2\}/Q\ ,$$
$$W_{\beta'}=2\gamma_3^{\beta'}\gamma_1\gamma_2(q^2+1)V_{23}^2/Q\ , \tag{A27}$$
$$W_\alpha=2\gamma_1\left[1+\gamma_2\frac{2qS+(q^2-1)P}{S^2+P^2}\right](A_1+A_3)-W_\beta-W_{\beta'}\ .$$

In the limit of a very weak ω_1 field, one may obtain z_1 and z_2 by solving the secular equation for the 2×2 submatrix of the effective Hamiltonian, involving the two states strongly mixed by the field E_2. In this limit one may verify that

$$A_1\cong 1\ ,$$
$$A_2\cong 0\ ,$$
$$A_3\cong 0\ ,$$

so that

$$W_\alpha\cong 2\gamma_1\left[1+\gamma_2\frac{2qS+(q^2-1)P}{S^2+P^2}\right]\ ,$$
$$W_\beta\cong 0\ , \tag{A28}$$
$$W_{\beta'}\cong 0\ .$$

[1]K. Shimoda, in *Laser Spectroscopy of Atoms and Molecules*, edited by H. Walther (Springer, Berlin, 1976).
[2]P. Lambropoulos and P. Zoller, Phys. Rev. A **24**, 379 (1981).
[3]K. Rzazewski and J. H. Eberly, Phys. Rev. Lett. **47**, 408 (1981); Phys. Rev. A **27**, 2026 (1983).
[4]A. Lami and N. K. Rahman, Phys. Rev. A **26**, 3360 (1982); **33**, 782 (1986); **34**, 3908 (1986); Opt. Commun. **43**, 383 (1982); in *Photons and Continuum States of Atoms and Molecules*, edited by N. K. Rahman, C. Guidotti, and M. Allegrini (Springer, Heidelberg, 1987), p. 62.
[5]P. T. Greenland, J. Phys. B **15**, 3191 (1982).
[6]M. Crance and L. Armstrong Jr., J. Phys. B **15**, 4637 (1982).

[7]L. I. Pavlov, S. S. Dimov, D. I. Mechikov, G. M. Mileva, K. V. Stamenov, and G. B. Altschuler, Phys. Lett. **89A**, 441 (1981); S. S. Dimov, L. I. Pavlov, K. V. Stamenov, Y. I. Heller, and A. K. Popov, Appl. Phys. B **30**, 35 (1983).

[8]P. Knight, Comments At. Mol. Phys. **15**, 193 (1984).

[9]K. S. Lam and T. F. George, Phys. Rev. A **33**, 2491 (1986).

[10]E. Kyrola, J. Phys. B **19**, 1437 (1986).

[11]S. L. Haan and G. S. Agarwal, Phys. Rev. A **35**, 4592 (1987).

[12]G. Alzetta, A. Gozzoni, L. Moi, and G. Orriols, Nuovo Cimento B **36**, 5 (1976); G. Alzetta, L. Moi, and G. Orriols, *ibid.* **52**, 209 (1979); E. Arimondo and G. Orriols, Nuovo Cimento Lett. **17**, 333 (1976); R. M. Whitley and C. R. Stroud, Phys. Rev. A **14**, 1498 (1976).

[13]H. Bachau, P. Lambropoulos, and R. Shakeshaft, Phys. Rev. A **34**, 4785 (1986).

[14]J. M. Bizau, D. Cubaynes, P. Gerard, F. J. Wuilleumier, J. L. Picque, D. L. Ederer, B. Carre, and G. Wendin, Phys. Rev. Lett. **97**, 306 (1986); Rapport d'Activité du Laboratoire pour l'Utilisation du Rayonnement Electromagnétique, Université de Paris–Sud, 1987 (unpublished).

[15]R. Pizzoferrato, M. Casalboni, R. Francini, U. M. Grassano, F. Antonangeli, M. Piacentini, N. Zena, and F. Bassani, Europhys. Lett. **2**, 571 (1986).

[16]R. Moccia and P. Spizzo, J. Phys. B **20**, 1423 (1987).

[17]D. E. Freund, B. D. Huxtable, and J. D. Morgan III, Phys. Rev. A **29**, 980 (1984).

[18]W. Shearer-Izumi, At. Data Nucl. Data Tables **20**, 531 (1977).

[19]L. Lipsky, R. Anania, and M. J. Conneely, At. Data. Nucl. Data. Tables **20**, 127 (1977).

[20]W. C. Martin, J. Phys. Chem. Ref. Data **2**, 257 (1973).